Nanocrystals

DOI: 10.1002/anie.201100983

Synthesis of Gold Nano-hexapods with Controllable Arm Lengths and Their Tunable Optical Properties**

*Do Youb Kim, Taekyung Yu, Eun Chul Cho, Yanyun Ma, O Ok Park, and Younan Xia**

Gold (Au) nanostructures have received considerable attention over the past decades because of their fascinating properties and applications.[1] For example, thanks to their versatility in surface modification, bio-inertness, and remarkable optical properties known as localized surface plasmon resonance (LSPR), Au nanostructures have recently been applied to various biomedical applications, such as cancer diagnosis/therapy, imaging, DNA analysis, and drug delivery.[2] In addition, Au nanostructures have been used as substrates for surface-enhanced Raman scattering (SERS), and most recently as heterogeneous catalysts.[3]

Since the properties of Au nanostructures can be tuned by controlling their morphologies, a rich variety of methods have been demonstrated for generating Au nanostructures with different morphologies, such as spheres, cubes, octahedra, decahedra, icosahedra, rods, plates, and stars.[4] Among them, branched or star-shaped Au nanostructures consisting of a core body and protruding arms have received particular interest due to their unique morphology and optical properties.[5] As shown both theoretically and experimentally, star-shaped Au nanostructures can exhibit strong enhancement of the electromagnetic field at the tips of their arms and also display a LSPR over a broad range of wavelengths.[5a–h] Thus, star-shaped Au nanostructures have been considered as a class of promising substrates for both SERS and LSPR applications. For these reasons, tremendous efforts have been devoted to the syntheses of star-shaped Au nanostructures. Most of the reported products were, however, characterized by random numbers of arms and broadly distributed arm lengths, and thus a poorly defined morphology.[5b–i] It remains a grand challenge to generate Au nanostructures with a branched morphology, and more importantly, an exact number of arms and controllable lengths.

Herein, we report a facile method for the synthesis of Au nano-hexapods by seeded growth, in which $HAuCl_4$ was reduced by *N*,*N*-dimethylformamide (DMF) in water in the presence of single-crystal Au octahedra. The newly formed Au atoms preferentially nucleated and grew from the six vertices of an octahedral seed, leading to the formation of a nano-hexapod. The LSPR peaks of the resultant Au nano-hexapods shifted from the visible (ca. 555 nm) to the near-infrared region (ca. 880 nm) depending on the lengths of the arms, which could be readily controlled by varying the amount of $HAuCl_4$, the reaction temperature, or both.

The single-crystal Au octahedra were prepared by seeded growth, in which Au spheres approximately 11 nm in diameter were directed to grow into octahedral nanocrystals by reducing $HAuCl_4$ with DMF at 80 °C in the presence of poly(vinyl pyrrolidone) (PVP).[6] As shown by the transmission electron microscopy (TEM) image in Figure S1 in the Supporting Information, Au octahedra with a uniform edge length of 24.5 nm could be routinely obtained with purity approaching 100 % without the involvement of any purification. In a typical synthesis of Au nano-hexapods (see the Supporting Information for details), the as-prepared suspension of Au octahedra was mixed with DMF and water in a vial, followed by the introduction of $HAuCl_4$ in DMF solution under magnetic stirring. After the reaction was allowed to proceed at room temperature (ca. 21 °C) for 5 h, the final product was collected by centrifugation, followed by washing with ethanol and water. Figure 1 a and b show scanning electron microscopy (SEM) and TEM images, respectively, of the Au nano-hexapods from a standard synthesis. It can be seen that the product displayed a highly branched morphology with an average size of approximately 60 nm as determined from the distance between two adjacent vertices. Figure 1 c shows a TEM image of a single hexapod at a higher magnification, clearly displaying an octahedral core and six arms on all the vertices. The average dimensions of the arms were 13.2 nm in width and 14.8 nm in length. The inset in Figure 1 c shows a proposed model of the nano-hexapod with an orientation similar to the structure displayed in the TEM image. Although there are some differences between the real hexapod and the proposed model due to the discrepancy in size and orientation of each arm, the model is a representation of the as-obtained nano-hexapod. We further confirmed the hexapod morphology by comparing the TEM images taken from the same nano-hexapod at different tilting angles with the proposed models at corresponding orientations. As shown in Figure S2 of the Supporting Information, the

[*] D. Y. Kim, Dr. T. Yu, Dr. E. C. Cho, Y. Ma, Prof. Y. Xia
Department of Biomedical Engineering, Washington University
Saint Louis, MO 63130 (USA)
E-mail: xia@biomed.wustl.edu
D. Y. Kim, Prof. O O. Park
Department of Chemical and Biomolecular
Engineering (BK21 graduate program)
Korea Advanced Institute of Science and Technology (KAIST)
291 Daehak-ro, Yuseong-gu, Daejeon 305-701 (Korea)

[**] This work was supported in part by the NSF (DMR-0804088) and startup funds from Washington University in St. Louis. As a visiting student from KAIST, D.Y.K. was also partially supported by the BK21 graduate program through the National Research Foundation of Korea funded by the Ministry of Education, Science and Technology. Part of the research was performed at the Nano Research Facility, a member of the National Nanotechnology Infrastructure Network (NNIN), which is supported by the NSF under award ECS-0335765.

Supporting information for this article is available on the WWW under http://dx.doi.org/10.1002/anie.201100983.

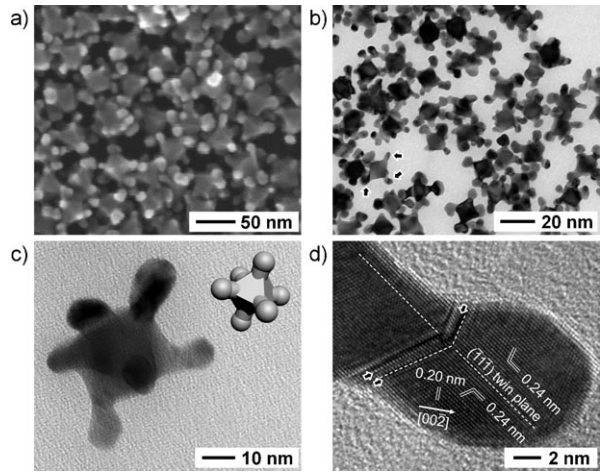

Figure 1. a) SEM and b) TEM images of Au nano-hexapods prepared with 24.5 nm Au octahedra as seeds and 10 μL of 9.42 mM $HAuCl_4$ at room temperature. c) TEM image of a single Au nano-hexapod at a higher magnification. The inset shows a model proposed for the Au nano-hexapod in the same orientation as the nanocrystal shown in the TEM image. d) HRTEM image taken at the boundary between the octahedral seed and one arm of the nano-hexapod.

nanostructures and proposed models match well at different tilting angles (see insets in Figure S2).

Interestingly, some additional contrasts appeared and then disappeared at the tips of an Au nano-hexapod when the sample was tilted, as marked by arrows in Figure S2. Similar contrasts were also observed at the tip portion of Au nano-hexapods when they were randomly oriented on a TEM grid, as marked by arrows in Figure 1 b. In general, these additional contrasts were observed when the Au nano-hexapods were sitting on the TEM grid with an orientation nearly along the [110] zone axis. Figure 1 d shows a typical high-resolution TEM image recorded from the tip portion of a single Au nano-hexapod sitting on the TEM grid along the [110] zone axis. Although this Au nano-hexapod was slightly tilted away from the [110] zone axis, the *d* spacing of 0.24 nm and 0.20 nm for adjacent lattice fringes could be indexed to the {111} and {100} planes of fcc Au, respectively (Figure 1 d). The high-resolution TEM study also revealed that there were some {111} twin planes (marked by arrows and dashed lines) in the structure, which seem to be responsible for the aforementioned contrasts at the tips of an Au nano-hexapod. We also observed a number of {111} twin plane and stacking faults parallel to the side face of an octahedral seed (see Figure S3 in the Supporting Information), characteristics that are very similar to what has been reported for platelike Au or Ag nanostructures.[7]

When the reduction rate is considerably slow, the formation of metal nanocrystals follows a kinetically controlled pathway, leading to the inclusion of stacking faults and other types of defects. The resultant metal nanocrystals typically take a shape deviated from those favored in terms of thermodynamic considerations.[8] The Au nano-hexapods were likely formed through a kinetically controlled process based on the following arguments: i) the concentration of $HAuCl_4$ was relatively low (15.2 μM); ii) the involvement of a relatively weak reducing agent at a moderately low concentration (DMF, ca. 10 % v/v); and iii) the use of a relatively low reaction temperature (room temperature, ca. 21 °C). The formation of a thermodynamically unfavorable shape like the Au nano-hexapod should have arisen from these reaction conditions, which could force the growth into a kinetically controlled process.

We could easily control the lengths of arms by varying the amount of $HAuCl_4$ added into the reaction system. Figure 2 shows TEM images of Au nano-hexapods prepared by using the standard procedure, except the volume of $HAuCl_4$. The sample obtained at a reduced volume for $HAuCl_4$ (1 μL, 1/10 of the standard procedure) showed a similar morphology, but the arms were much shorter (Figure 2 a). The octahedral core apparently did not change much in size relative to the octahedral seeds (29.6 nm), whereas the average overall size was increased to 33.4 nm. This result indicates that most of the newly formed Au atoms were deposited preferentially onto the six vertices of the octahedral Au seed, leading to the formation of a nano-hexapod with very short (ca. 2.0 nm) arms (more like tips). When the volume of $HAuCl_4$ was increased from 1 to 5 μL (1/2 of what was used in the standard procedure), the average length of arms and the overall size of resultant Au nano-hexapods were 5.9 nm and 40.9 nm, respectively, while the size of the octahedral core remained roughly the same. As shown in Figure S4a in the Supporting Information, the average overall sizes of the Au nano-hexapods and the lengths of their arms were linearly increased from 33.4 nm to 60.0 nm and 2.0 nm to 14.8 nm, respectively, as the volume of $HAuCl_4$ was increased from 1 μL to 10 μL. However, when the volume of $HAuCl_4$ was further increased to 20 μL, the overall size of the Au nano-hexapods and their arms only increased marginally as compared to those obtained with 10 μL of $HAuCl_4$. This observation indicates that the octahedral seed grew preferentially along the six vertices in the early stage and then switched to other directions. As shown in Figure 2 c and d, the Au nano-hexapods obtained with 20 μL and 30 μL of $HAuCl_4$

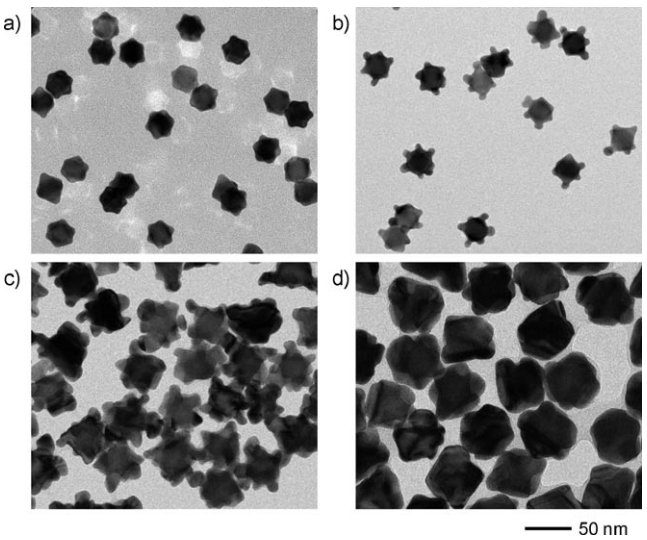

Figure 2. TEM images of Au nanocrystals obtained under the same reaction conditions as those for Figure 1 (the standard synthesis), except the change of $HAuCl_4$ volume from 10 μL to: a) 1 μL, b) 5 μL, c) 20 μL, and d) 30 μL, respectively.

were slightly larger than those in Figure 1, but showed much reduced lengths for the arms. In fact, the Au nano-hexapods obtained with 30 μL $HAuCl_4$ were nearly octahedral in shape, but with concaved facets and edges (see Figure S6 in the Supporting Information). The morphological changes as a function of $HAuCl_4$ concentration can be attributed to the slight truncation at the corners of an octahedral Au seed, and therefore the exposure of {100} facets at its vertices (see Figure S1 in the Supporting Information).[6] The relatively higher surface energy of {100} than {111} facets of an octahedral seed could lead to the preferential deposition of newly formed Au atoms on the six vertices of an octahedral seed and the resultant tips could grow longer as long as the synthesis was kept under kinetically controlled conditions. However, the quick increase in total surface energy may force the nano-hexapod to evolve into a thermodynamically favorable shape like an octahedron by reducing the longitudinal growth rate along the arms.

We could also control the lengths of arms by changing the reaction temperature. Figure 3 shows TEM images of the Au nano-hexapods obtained by using the standard procedure, but at various reaction temperatures. The Au nanocrystals obtained at elevated temperatures up to 80 °C still exhibited a branched morphology with six arms at the vertices. As the reaction temperature was increased, the lengths of the arms decreased. The average arm lengths of the Au nano-hexapods were 12.9, 11.2, and 8.8 nm, respectively, when the reaction temperature was 40, 60, and 80 °C. The overall sizes and arm lengths of the Au nano-hexapods obtained at different reaction temperatures are displayed in Figure S4b in the Supporting Information, which suggests a linear relationship between the arm length of the Au nano-hexapods and the reaction temperature. It should be emphasized that the three samples shown in Figure 3 were obtained with the same amount of $HAuCl_4$, implying that Au atoms of roughly the same number were deposited on the octahedral seed. When comparing the samples obtained at different reaction temperatures, it can be seen that the Au nano-hexapods obtained at a higher reaction temperature had slightly larger cores than those obtained at a lower reaction temperature. It seems to be that an increase in reduction rate due to an increase of the reaction temperature could promote lateral growth on the octahedral seed and thus shorten the lengths of the arms of resultant Au nano-hexapods. On the other hand, the Au nano-hexapods with longer arms are thermodynamically less favorable, and they tended to evolve into Au nano-hexapods with shorter arms at an elevated reaction temperature.

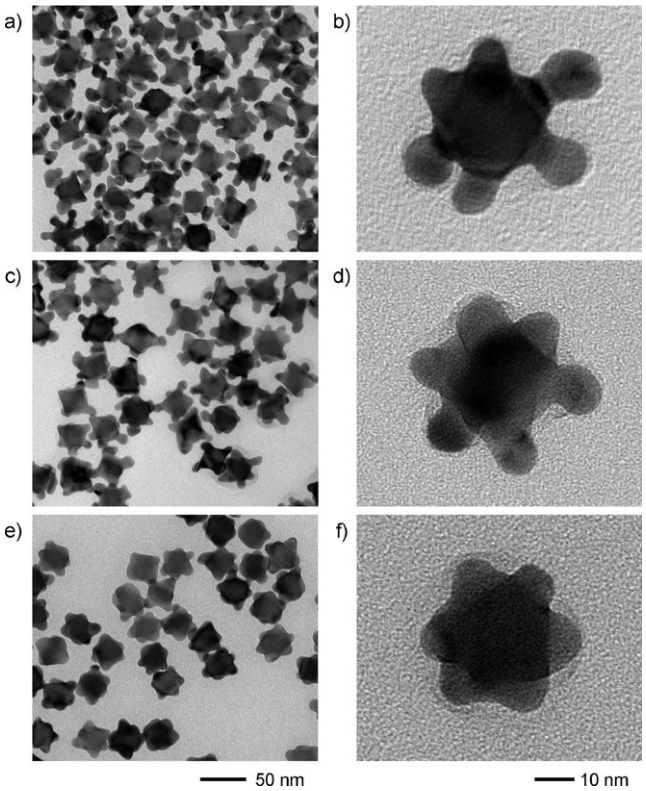

Figure 3. Low-magnification (left panel) and high-magnification (right panel) TEM images of Au nano-hexapods obtained under the same reaction conditions as those for Figure 1, except the use of different reaction temperatures: a, b) 40 °C, c, d) 60 °C, and e, f) 80 °C, respectively.

We further characterized the optical properties of the Au nano-hexapods using UV-Vis-NIR spectroscopy. Despite their structural complexity, suspensions of the Au nano-hexapods showed well-defined LSPR features. Figure 4a shows extinction spectra of the Au octahedral seeds and the nano-hexapods produced by using different volumes of $HAuCl_4$ at room temperature. Similar to star-shaped Au nanocrystals,[5b] the nano-hexapods displayed two distinct LSPR peaks that can be assigned to the dipolar resonances localized at either the tips or the central core. Significantly, the peak position of the main, longitudinal resonance mode corresponding to the tip-localized mode[5b] could be continuously red-shifted from 579 nm to 880 nm as the volume of $HAuCl_4$ was increased to 10 μL. However, as the volume of $HAuCl_4$ was further increased, the main LSPR band was blue-shifted and the Au nano-hexapods only exhibited one single LSPR peak at 580 nm when the volume of $HAuCl_4$ was increased to 30 μL. These results are consistent with the morphological changes observed by TEM imaging (Figure 1 and Figure 2). When the volume of $HAuCl_4$ was increased to 10 μL, the arms of the Au nano-hexapods were increased in length, causing their main LSPR peak to red-shift. When the volume of $HAuCl_4$ was increased to 20 μL, the length of their arms was roughly the same as those obtained with 10 μL of $HAuCl_4$, but their aspect ratio was reduced due to lateral growth, causing their main LSPR peak to blue-shift. The single intense peak at 580 nm observed for the Au nanocrystals obtained with 30 μL of $HAuCl_4$ could be attributed to their nearly octahedral shape, which was also in good agreement with the LSPR peak position expected for Au octahedra with a similar size.[6,9] Although the peak position of the main LSPR band was greatly shifted as the morphology was changed, the position of the LSPR band corresponding to the core[5b] only showed marginal shifts around 530 nm: for example, it was only blue-shifted by approximately 25 nm relative to that of the octahedral seeds. The octahedral seed could be considered as a truncated octahedron in the core after arms had grown on their vertices because some of the newly formed Au atoms were also deposited on the side faces in addition to the vertices (see Figure S7 in the Supporting

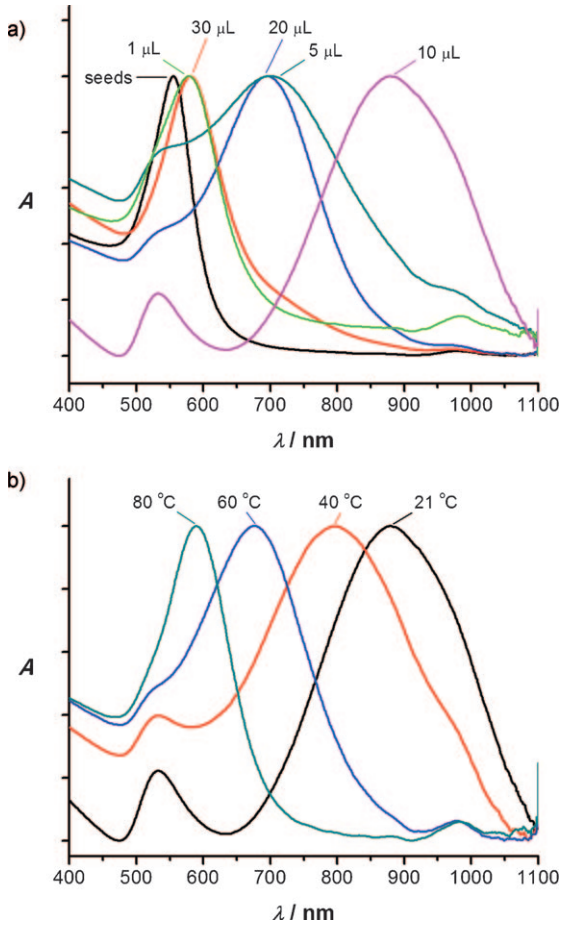

Figure 4. UV-Vis-NIR absorption spectra taken from a) Au octahedra used as seeds and the Au nano-hexapods obtained with different volumes of $HAuCl_4$ and b) the Au nano-hexapods obtained at different reaction temperatures. The samples were suspended in ethanol.

Information). As shown in our previous work, the LSPR peak of a Au octahedron would be blue-shifted when its corners and edges were truncated.[6,10]

The Au nano-hexapods obtained at different reaction temperatures also showed similar trends of shift for the LSPR peaks. The peak position of the main LSPR band was continuously blue-shifted from 880 nm to 590 nm as the reaction temperature was increased from room temperature (ca. 21 °C) to 80 °C and there was a more or less linear relationship between the main LSPR peak position and the reaction temperature (see Figure 4b and Figure S8 in the Supporting Information). In comparison with the corresponding TEM images of the Au nano-hexapods shown in Figure 1 and Figure 3, the blue shift could be attributed to the shortening of the arms for the nano-hexapods as the reaction temperature was increased. Although the core size of the nano-hexapod was also slightly increased as the reaction temperature was increased, the increase was insufficient to cause any major shift in the position of the core mode, which was essentially unchanged at approximately 530 nm.

In summary, we have demonstrated a facile method based on seeded growth for the synthesis of Au nano-hexapods with a well-defined morphology, as well as uniform and controllable sizes. The success of this kinetically controlled growth can be attributed to the mild reaction conditions such as low concentrations of seeds and Au ions, relatively low reaction temperatures, and weak reducing power; all of these conditions were pivotal to the formation of a thermodynamically unfavorable shape such as the Au nano-hexapod. Furthermore, the arm lengths of the Au nano-hexapods (and thus their optical properties) could be readily controlled by changing the volume of $HAuCl_4$ added into the reaction system and/or the reaction temperature. These Au nano-hexapods can be used as active substrates for SERS and LSPR and this approach may provide a simple route to the synthesis of metal nanocrystals with a branched and yet well-defined morphology.

Received: February 8, 2011
Published online: June 6, 2011

Keywords: gold · hexapods · nanocrystals · nanostructures · seeded growth

[1] a) M.-C. Daniel, D. Astruc, *Chem. Rev.* **2004**, *104*, 293; b) M. Hu, J. Chen, Z.-Y. Li, L. Au, G. V. Hartland, X. Li, M. Marquez, Y. Xia, *Chem. Soc. Rev.* **2006**, *35*, 1084.

[2] a) D. A. Giljohann, D. S. Seferos, W. L. Daniel, M. D. Massich, P. C. Patel, C. A. Mirkin, *Angew. Chem.* **2010**, *122*, 3352; *Angew. Chem. Int. Ed.* **2010**, *49*, 3280; b) E. Boisselier, D. Astruc, *Chem. Soc. Rev.* **2009**, *38*, 1759; c) J. J. Storhoff, A. D. Lucas, V. Garimella, Y. P. Bao, U. R. Müller, *Nat. Biotechnol.* **2004**, *22*, 883.

[3] a) A. S. K. Hashmi, G. J. Hutchings, *Angew. Chem.* **2006**, *118*, 8064; *Angew. Chem. Int. Ed.* **2006**, *45*, 7896; b) S. Eustis, M. A. El-Sayed, *Chem. Soc. Rev.* **2006**, *35*, 209.

[4] a) C. Burda, X. Chen, R. Narayanan, M. A. El-Sayed, *Chem. Rev.* **2005**, *105*, 1025; b) M. Grzelczak, J. Pérez-Juste, P. Mulvaney, L. M. Liz-Marzán, *Chem. Soc. Rev.* **2008**, *37*, 1783; c) A. R. Tao, S. Habas, P. Yang, *Small* **2008**, *4*, 310.

[5] a) C. L. Nehl, H. Liao, J. H. Hafner, *Nano Lett.* **2006**, *6*, 683; b) P. Senthil Kumar, I. Pastoriza-Santos, B. Rodríguez-González, F. J. García de Abajo, L. M. Liz-Marzán, *Nanotechnology* **2008**, *19*, 015606; c) S. Barbosa, A. Agrawal, L. Rodríguez-Lorenzo, I. Pastoriza-Santos, R. A. Alvarez-Puebla, A. Kornowski, H. Weller, L. M. Liz-Marzán, *Langmuir* **2010**, *26*, 14943; d) C. G. Khoury, T. Vo-Dinh, *J. Phys. Chem. C* **2008**, *112*, 18849; e) E. N. Esenturk, A. R. H. Walker, *J. Raman Spectrosc.* **2009**, *40*, 86; f) G. H. Jeong, Y. W. Lee, M. Kim, S. W. Han, *J. Colloid Interface Sci.* **2009**, *329*, 97; g) J. Xie, Q. Zhang, J. Y. Lee, D. I. C. Wang, *ACS Nano* **2008**, *2*, 2473; h) F. Hao, C. L. Nehl, J. H. Hafner, P. Nordlander, *Nano Lett.* **2007**, *7*, 729; i) J. Xie, J. Y. Lee, D. I. C. Wang, *Chem. Mater.* **2007**, *19*, 2823.

[6] D. Y. Kim, W. Li, Y. Ma, T. Yu, Z.-Y. Li, O O. Park, Y. Xia, *Chem. Eur. J.* **2011**, *17*, 4759.

[7] a) V. Germain, J. Li, D. Ingert, Z. L. Wang, M. P. Pileni, *J. Phys. Chem. B* **2003**, *107*, 8717; b) C. Lofton, W. Sigmund, *Adv. Funct. Mater.* **2005**, *15*, 1197; c) J. Zeng, S. Roberts, Y. Xia, *Chem. Eur. J.* **2010**, *16*, 12559.

[8] a) Y. Xia, Y. Xiong, B. Lim, S. E. Skrabalak, *Angew. Chem.* **2009**, *121*, 62; *Angew. Chem. Int. Ed.* **2009**, *48*, 60; b) Y. Xiong, A. R. Siekkinen, J. Wang, Y. Yin, M. J. Kim, Y. Xia, *J. Mater. Chem.* **2007**, *17*, 2600.

[9] C. Li, K. L. Shuford, M. Chen, E. J. Lee, S. O. Cho, *ACS Nano* **2008**, *2*, 1760.

[10] D. Y. Kim, S. H. Im, O O. Park, Y. T. Lim, *CrystEngComm* **2010**, *12*, 116.

